Physica B 404 (2009) 2517–2519

Contents lists available at ScienceDirect

Physica B

journal homepage: www.elsevier.com/locate/physb

Neutron polarization analysis on the multiferroic $TbMn_2O_5$

L.J. Chang [a,*], Y. Su [b], W. Schweika [c], Th. Brückel [b,c], Y.Y. Chen [d], D.S. Jang [e], R.S. Liu [e]

[a] Nuclear Science and Technology Development Center, National Tsing Hua University, Hsinchu 30013, Taiwan
[b] Jülich Centre for Neutron Science (JCNS), Institut für Festkörperforschung, Forschungszentrum Jülich, Outstation at FRM-II, Lichtenbergstrasse 1, D-85747 Garching, Germany
[c] Institut für Festkörperforschung, Forschungszentrum Jülich, D-52425 Jülich, Germany
[d] Institute of Physics, Academia Sinica, Nankang Taipei 115, Taiwan
[e] Department of Chemistry and Center for Nano Storage Research, National Taiwan University, Taipei 106, Taiwan

ARTICLE INFO

Keywords:
Multiferroics
Neutron diffraction
Specific heat

ABSTRACT

Polycrystalline $TbMn_2O_5$ was prepared by the standard solid-state reaction method and characterized by powder X-ray diffraction and magnetization to assure it is of single phase. Heat capacity measurements on the compound reveal an antiferromagnetic phase transition at ~45 K. A broad peak below ~6 K in the heat capacity measurements corresponds to the crossover transition of Tb^{3+} ordering. To confirm these magnetic orderings, neutron powder diffractions on $TbMn_2O_5$ with XYZ neutron polarization analysis were performed at the diffuse neutron scattering (DNS) spectrometer, FRJ-II, by using neutron wavelength of 4.8 Å in the temperature range of 1.8–250 K. Magnetic scattering was separated from nuclear coherent and spin incoherent scattering contributions. Long-range ordered magnetic peaks were observed below ~39 K which is consistent with the heat capacity results. The drastic increasing intensities below ~6 K indicate the ferromagnetic transition in Tb^{3+} orderings.

There is currently a great interest in the materials that exhibit interplay between lattice distortions and electrical and magnetic ordering. Among these materials, magnetoelectrics or multiferroics, in which magnetism and ferroelectricity coexist and are mutually coupled, are being investigated extensively. Multiferroics display phenomena such as the control of electrical polarization by the application of an external magnetic field, providing an additional degree of freedom for the design of new devices [1]. Nevertheless, these materials include compounds of very different crystallographic structures, such as kagomé staircase $Ni_3V_2O_8$ [2], spinel $CoCr_2O_4$ [3], hexagonal $Ba_{0.5}Sr_{1.5}Zn_2Fe_{12}O_{22}$ [4], the perovskite $REMnO_3$ (RE = Gd, Tb, Dy) [5], and orthorhombic $REMn_2O_5$ (RE = Tb, Ho, Dy) [6]. Although these compounds only have values of the electric polarization two orders of magnitude smaller than those in the traditional ferroelectrics, they provide opportunities for theoretical realizations of the new mechanism of magnetoelectric coupling [7]. The experimental results on these materials indicated that the helical magnetic structures may be a means to host ferroelectricity [7], and the so-called E-type magnetic order had been proposed as the deviation of ferroelectricity in $HoMnO_3$ [8]. In $REMn_2O_5$, either a nearly collinear acentric magnetic order with broken inversion symmetry [9] or a spiral spin configuration along the Mn^{4+} spin chain [10] were proposed to explain the ferroelectricity in the compounds. These suggest that the mechanism leading to the multiferrocity in $REMn_2O_5$ is still uncertain. In addition, compounds showing large magnetoelectric effects are extremely rare. The magnetoelectric $TbMn_2O_5$ exhibits a profound interplay between electrical polarization and the applied magnetic field. This is evidenced by two observed facts in the compound, the highly reversible switching of electrical polarization using relatively low magnetic fields of 0–2 T; and the combined application of electric and magnetic field, which leaves a permanent imprint in the polarization [6]. Neutron polarization analysis on the neutron diffraction provides a unique technique to probe and separate the different intensity contributions from the nuclear and magnetism. In this paper we will show the results of neutron polarization analysis applied to $TbMn_2O_5$.

$TbMn_2O_5$ is an insulator and consists of linked $Mn^{4+}O_6$ octahedra and $Mn^{3+}O_5$ pyramids adopting space group Pbam. The octahedral shares edges to form ribbons parallel to the *c* axis, adjacent ribbons being linked by pairs of corner-sharing pyramids [1]. The structure at room temperature is orthorhombic [11]. Neutron diffraction experiments on $TbMn_2O_5$ as a function of temperature and applied field show unambiguous correlations between dielectric anomalies and changes in the periodicity of the spin structure [12]. At 38 K, the onset of ferroelectricity is related to the occurrence of incommensurate antiferromagnetic ordering at $T_1 = 43$ K. When the temperature is just above the maximum in spontaneous polarization **P** at $T_2 = 33$ K, propagation vector **k** locks into a commensurate value $(\frac{1}{2}, 0, \frac{1}{4})$. Furthermore, at $T_3 = 24$ K, where the dielectric constant ε has an upward peak,

* Corresponding author. Tel.: +886 3 5742863; fax: +886 3 5713849.
E-mail address: ljchang@mx.nthu.edu.tw (L.J. Chang).

0921-4526/$ - see front matter © 2009 Elsevier B.V. All rights reserved.
doi:10.1016/j.physb.2009.06.011

k becomes suddenly incommensurate again. It is an unusual example of such a transition on cooling. The low temperature transition ($T_4 = 10$ K) is consistent with a major increase in the Tb ordered moment. The 43 and 24 K transitions are accompanied by clear anomalies in the lattice parameters, particularly along the *b* "polar" axis, and in the atomic displacement parameters [12].

$TbMn_2O_5$ polycrystalline sample has been prepared by a conventional solid-state reaction method. The powder X-ray diffraction confirms the sample to be single phase, and the lattice constants were calculated as $a\sim7.34$ Å, $b\sim8.53$ Å, and $c\sim5.65$ Å. The magnetization measured by SQUID magnetometer at applied field 100 G is shown in Fig. 1.

A broad peak has been observed on the magnetic susceptibility in the temperature range of 50–20 K, which corresponds to the series of transitions mentioned above. A linear fit on $1/\chi$ above temperature 150 K shows the Curie temperature being ~30 K, and the system is antiferromagnetic. The total effective moment was estimated as $\sim17.2\mu_B$. The value is very close to the summation of Tb^{3+}, Mn^{3+}, and Mn^{4+} free moments. However, no obvious Tb^{3+} long range order was observed in the magnetization measurements down to 2 K. Specific heat measurements were carried out using a thermal relaxation method down to 0.5 K. The results for C/T vs. T are exhibited in Fig. 2. The anomalies at 38 and 25 K correspond to the magnetically induced ferroelectricity and the Mn^{3+}/Mn^{4+} spin reorientation in the system, respectively [6]. The sharp peak at 43 K reveals long-range antiferromagnetic ordering of Mn^{3+}/Mn^{4+}, which was suggested to be the cause driving the ferroelectric transition at 38 K through the Jahn–Teller distortion [6]. The inset in Fig. 2 illustrates the low temperature configuration of specific heat C vs. T below 10 K. A broad peak centered at 2 K and rising below 6 K was observed. This may suggest the slow frozen process on Tb^{3+}. Hur et al. indicated that the significant C rise below 10 K on cooling may suggest the slow onset of Tb magnetic order [6].

Neutron scattering experiments with neutron polarization analysis were performed at DNS, FRJ-II to distinguish the scattering contributions from nuclear and magnetism. Neutron wavelength 4.8 Å was chosen for all the diffraction experiments. A closed-cycle cryostat was used for temperature control between 250 and 1.8 K. The spectrometer DNS is similar to the instrument D7 at ILL, Grenoble, but has a comparably compact design. The polarizers and analyzers are made of a stack of sputtered magnetic supermirrors. The polarizers have a geometrical design of a focusing bender to focus beam on the sample with a substantial gain in neutron intensity. The main detector bench with 50 units is for unpolarized experiments and a second detector bench with 12 detector units, which are equipped with supermirror benders as analyzers, are used for polarization analysis. The xyz coils around the sample are installed to change the neutron polarization directions adiabatically on the path to and from the sample. The standard three-directional polarization analysis method [13] was used for separating different scattering contributions. For considering nuclear scatterings only, the contributions of coherent nuclear- and spin-incoherent scatterings can be derived from the spin-flip and non-spin flip scatterings. By a field variation perpendicular and parallel to the scattering vector **Q**, the magnetic scattering contribution can be separated out from the nuclear contributions since the coherent nuclear scattering and spin-incoherent scatterings are independent of the magnetic field [14]. The details of the neutron polarization analysis method can be referred from Ref. [15].

Fig. 3 shows the separated spectra of coherent nuclear, spin-incoherent nuclear and magnetic scattering by neutron polarization analysis at the temperature of 1.8 K.

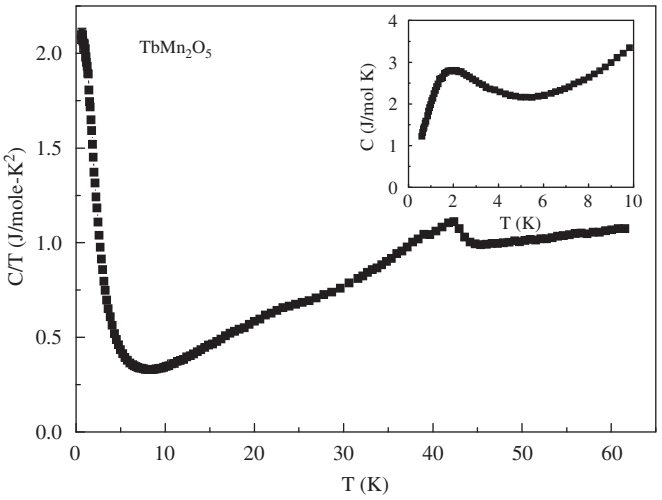

Fig. 2. Specific-heat C/T vs. T for $TbMn_2O_5$. The inset illustrates the low temperature behavior of specific heat C vs. T below 10 K.

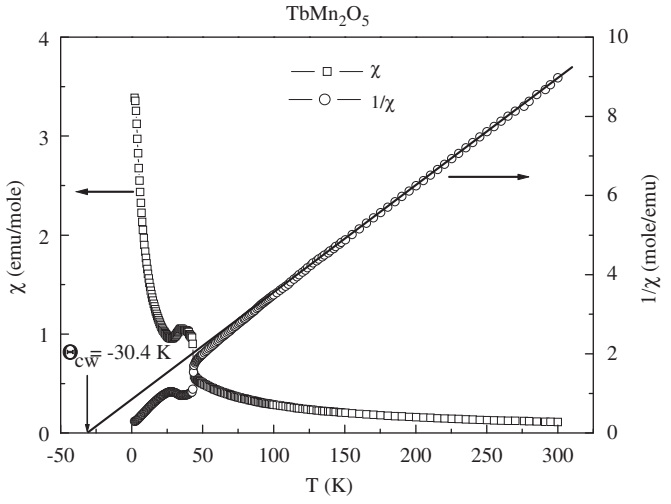

Fig. 1. Magnetization measurements at the applied field 100 G, and the temperature dependence of inverse magnetic susceptibility $1/\chi$ for $TbMn_2O_5$. The Curie temperature was estimated as ~30 K, and the total effective moment $\sim17.2\mu_B$.

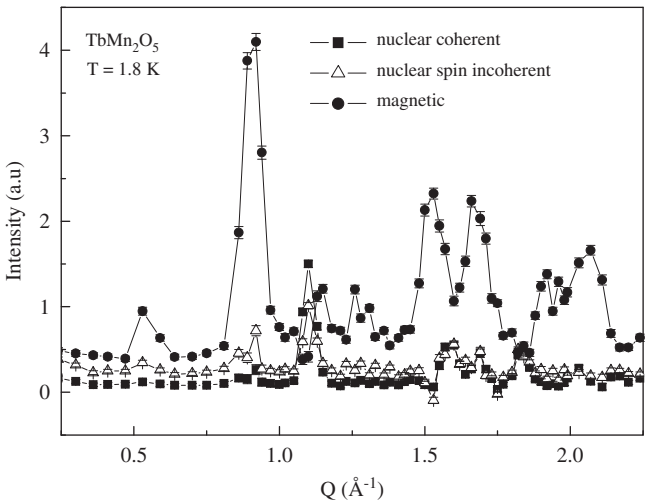

Fig. 3. The separation of coherent nuclear, spin-incoherent nuclear and magnetic scattering at 1.8 K. The intensities were normalized to the performance of each detector.

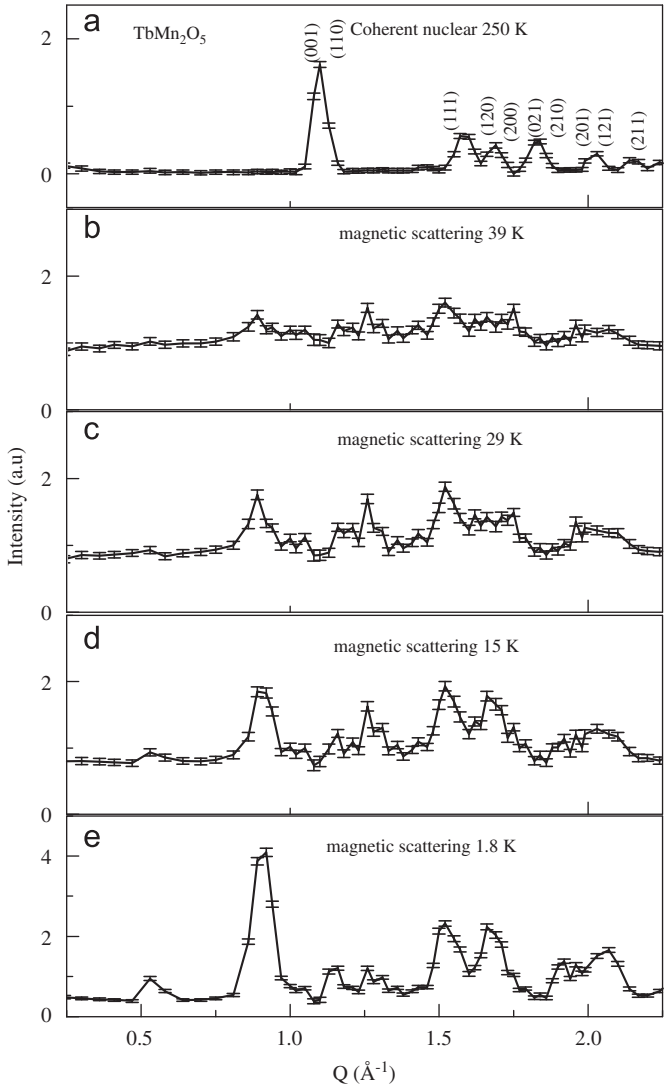

Fig. 4. (a) The coherent nuclear scattering at 250 K, and the magnetic scatterings at (b) 39 K, (c) 29 K, (d) 15 K, and (e) 1.8 K.

The efficiency of each detector and polarization analyzer was calibrated by the spin-incoherent scattering of a standard vanadium sample. The background for magnetic scattering indicates that the magnetic moments are partially ordered even down to 1.8 K. This is consistent with our specific heat results in Fig. 2. As the standard xyz-separation applies only for powders of collinear AF or paramagnets [13], the complex magnetic structure will probably cause systematic deviations. This is evident from the nuclear spin-incoherent scattering which must be the same for all temperature range. For 15 K and lower T the nuclear spin-incoherent contribution appears to be much higher than at higher T (not shown in the figure); we thus concluded that the difference must come from magnetic scattering. A similar behavior can be seen in the nuclear coherent scattering. The residue intensities and the peaks at $Q\sim0.8\,\text{Å}^{-1}$ in nuclear coherent and spin-incoherent spectra in Fig. 3 are presumed not nuclear but of magnetic origin due to insufficient separation, because this peak was only observed below the Mn^{3+}/Mn^{4+} ordering temperature ~40 K, and the intensity increases when the temperature decreases. This may be due to either not perfect corrections for flipping ratio background and multiple scattering and/or it may have a cause also in the complex non-collinear structure. However, a single crystal sample is necessary for the further neutron diffuse scattering studies on the Tb^{3+} partially ordered state.

Fig. 4(a) shows the coherent nuclear scattering spectra at 250 K. The magnetic scattering spectra at 39, 29, 15, and 1.8 K are exhibited in Fig. 4(b–e), respectively. The increase of magnetic peak intensities from high to low temperatures is consistent with the decrease in paramagnetic background. The magnetic peaks can be indexed as (h/2, k, l$\pm$0.3) approximately which is consistent with the results of Gardner et al. [16]. More details studied by magnetic neutron diffraction [17] and polarized soft-X-ray magnetic scattering [18,19] reveal that the magnetic scatterings in this compound are complex. The commensurate magnetic phase with the propagation vector $(\frac{1}{2},0,\frac{1}{4})$ was observed between 37 and 22 K, and the incommensurate magnetic phase propagation vectors varied with temperatures above 37 K and below 22 K. However, those modulations were not observed under our current experimental resolutions. Single crystals have been prepared in order to observe the magnetic diffuse scatterings in different temperature ranges. This information would correspond to the complex magnetic correlations in the compound, and thus reveals the interactions between polarization and magnetism which is still unclear in the multiferroics.

For summary, we prepared a polycrystalline sample of $TbMn_2O_5$ and studied magnetic and structural properties. The system was estimated to have the Curie temperature ~30 K, and the total effective moment was estimated as $\sim17.2\mu_B$ which is very close to the summation of Tb^{3+}, Mn^{3+}, and Mn^{4+} free moments. The broad peak rising below 6 K on cooling in specific heat measurement reveals the slow onset of Tb magnetic order. Neutron polarization analysis was carried out on DNS, FRJ-II, to separate the spectra of nuclear coherent, nuclear spin-incoherent and magnetic contributions. Paramagnetic background in the magnetic scattering was observed below 1.8 K. It indicates the system is partially ordered at these temperatures.

Acknowledgements

This work was supported by the National Science Council, Taiwan, Republic of China under the project number NSC 96-2739-M-213-001.

References

[1] G.R. Blake, et al., Phys. Rev. B 71 (2005) 214402.
[2] G. Lawes, et al., Phys. Rev. Lett. 95 (2005) 087205.
[3] Y. Yamasaki, et al., Phys. Rev. Lett. 96 (2006) 207204.
[4] T. Kimura, et al., Phys. Rev. Lett. 71 (2005) 224425.
[5] T. Kimura, et al., Nature (London) 426 (2004) 55.
[6] N. Hur, et al., Nature (London) 429 (2004) 392.
[7] I.A. Sergienko, et al., Phys. Rev. B 73 (2006) 094434.
[8] I.A. Sergienko, et al., Phys. Rev. Lett. 97 (2006) 227204.
[9] L.C. Chapon, et al., Phys. Rev. Lett. 96 (2006) 097601.
[10] Y.J. Choi, et al., Phys. Rev. Lett. 100 (2008) 047601 and the references therein.
[11] D. Higashiyama, et al., Phys. Rev. B 72 (2005) 064421.
[12] L.C. Chapon, et al., Phys. Rev. Lett. 93 (2004) 177402.
[13] O. Schärpf, et al., Phys. Stat. Sol. A 135 (1993) 359.
[14] G. Shirane, et al., Phys. Rev. B 31 (1985) 1227.
[15] Th. Brückel, W. Schweika (Eds.), Polarized Neutron Scattering, Forschungszentrum, Jülich, 2002.
[16] P.P. Gardner, et al., J. Phys. C 21 (1988) 5653.
[17] S. Kobayashi, et al., J. Phys. Soc. Jpn. 73 (2004) 3439.
[18] J. Okamoto, et al., Phys. Rev. Lett. 98 (2007) 157202.
[19] J. Koo, et al., Phys. Rev. Lett. 99 (2007) 197601.